Formation of Silver Nanoparticles under Structured Amino Groups in Pseudo-dendritic Poly(allylamine) Derivatives

Ping-Lin Kuo* and Wei-Fu Chen

Department of Chemical Engineering, National Cheng Kung University, Tainan, Taiwan 70101, ROC

Received: January 28, 2003; In Final Form: May 21, 2003

The syntheses of silver nanoparticles stabilized by poly(allylamine) (PAA) and by polyethyleneiminated poly(allylamine) (PAA(EI)$_n$ (n = 2, 5.8)) are reported. The architectural effects in particle on the nanoparticle size, size distribution, and agglomeration behavior are determined from the UV−vis plasmon absorption band and transmission electron microscopic (TEM) analyses. The data show that PAA(EI)$_n$ display better stabilizing effects than PAA to prevent silver particles from agglomeration. Different phenomena of the polymer-protected nanoparticles at various silver ion concentrations are observed and are explained in terms of a mechanism of structure-dependent stabilization.

Introduction

The preparation of metal nanoparticles is a major research area in nanoscale science and engineering. A better strategy to generate uniform particles is to undergo chemical reduction via microemulsion,[1,2] coprecipitation,[3−5] polymer protection,[6,7] and so on.[8−10] The purpose of these methods is to control the size and polydispersity of particles through reducing the surface energy by means of the adsorption of stabilizers such as polymeric ligands or surfactants. The stabilizing effect of these macromolecules is attributable to the fact that either the small particles are attached to the much larger protecting polymers or the protecting molecules cover or encapsulate the metal particles. Dendrimer molecules with a well-defined structure have been used as templates to host inorganic nanoparticles as reported by Balogh's group[11] and Crooks' group.[12] Even though this method possesses advantages of simplicity and efficiency, it has been reported that the preparation of silver nanoparticles within dendrimers results in precipitation from solution after a short time without repeatability in UV−vis absorption spectra.[12b] Consequently Crooks' group and Esumi's group demonstrated the concept that larger metal particles (2−3 nm) can be protected by the exterior amine groups of dendrimers which act as stabilizers for the most part.[13] Very recently, the studies of Manna et al.[14] have refined this model, and vary stable silver nanoparticles passivated by the terminal amino groups of dendrimers have been prepared successfully.

In our previous work, water-soluble polymers grafted or terminated with hyperbranched poly(ethyleneimine) have been synthesized to study their chelating characteristics to metal ions.[15] In the present paper, silver nanoparticles are prepared by direct reduction of metal salt with $NaBH_4$ in the presence of pseudo-dendritic polymers poly(ethyleneiminated) poly(allylamine) (PAA(EI)$_n$) and comparable polymers poly(allylamine) (PAA). The hyperbranched polymers possess high densities of amine functionalities and act as highly effective polymeric chelating agents. Stable silver nanoparticles are successfully obtained in aqueous solution without precipitates by the same procedures as Crooks and Esumi demonstrated. The features of silver particles prepared under different protectors are compared to explore the effects of polymer architecture on the nanoparticle formation. Our findings indicate that poly(allylamine) provides poor stabilization leading to agglomeration of nanoparticles; however, poly(ethyleneiminated) poly(allylamine) displays excellent protecting effects.

CHART 1

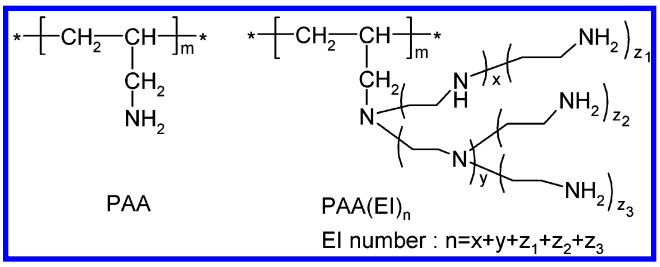

Experimental Section

Materials. Poly(allylamine) [weight-average molecular weight (M_w), 10 000] was supplied from Nitto Boseki Co.. Poly(ethyleneiminated) poly(allylamine) with different ethyleneimine numbers (EI number n = 2, 5.8) were synthesized by a simple *in situ* ethylamination of PAA with 2-chloroethylamine hydrochloride following the procedures as described in our previous works.[15] Fresh aqueous solutions of silver nitrate (Acros) were prepared for every synthesis. Sodium borohydride (Lancaster) was used as received. The water used throughout all experiments was purified through a Milli-Q system.

Preparation of PAA(EI)$_n$-Protected Silver Particles. The chemical structures of PAA and PAA(EI)$_n$ are shown in Chart 1, where n is the average number of ethyleneimine groups per repeating amino group on the polymer backbone (n = 2 and 5.8). [N] is defined as the total normality concentration of amino groups on PAA or PAA(EI)$_n$.

The synthesis procedure of silver nanoparticles is similar to that reported by Crooks and co-workers.[13,16] Typically, 10 mL of 1 mM [N] of PAA(EI)$_n$ and 0.1 mM Ag^+ solution was prepared, followed by adding 3×10^{-3} μmol of sodium

* To whom all correspondence should be addressed. Telephone: +886-6-275 7575-62658. Fax: +886-6-276 2331. E-mail: plkuo@mail.ncku.edu.tw.

10.1021/jp030116s CCC: $25.00
Published on Web 09/24/2003

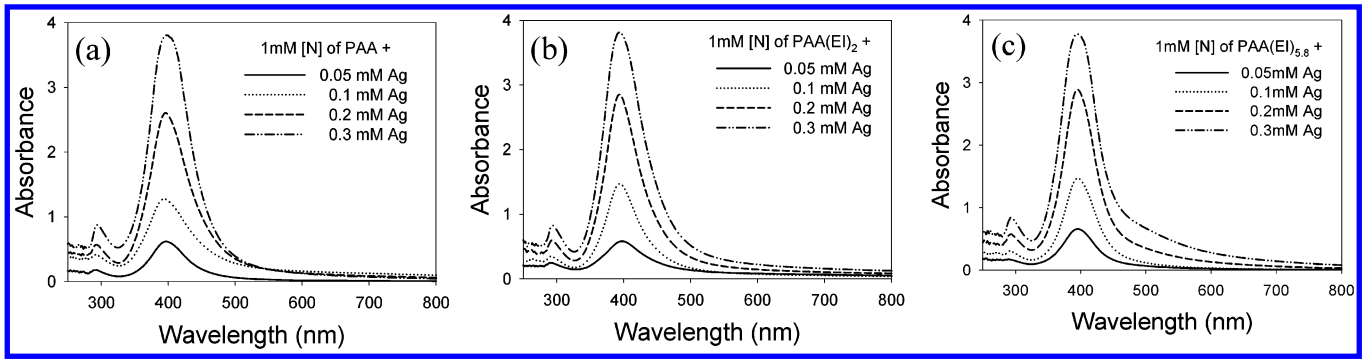

Figure 1. UV−vis spectra of variant concentrations of Ag^+ in the presence of (a) 1 mM [N] of PAA, (b) 1 mM [N] of $PAA(EI)_2$, and (c) 1 mM [N] of $PAA(EI)_{5.8}$ after reduction.

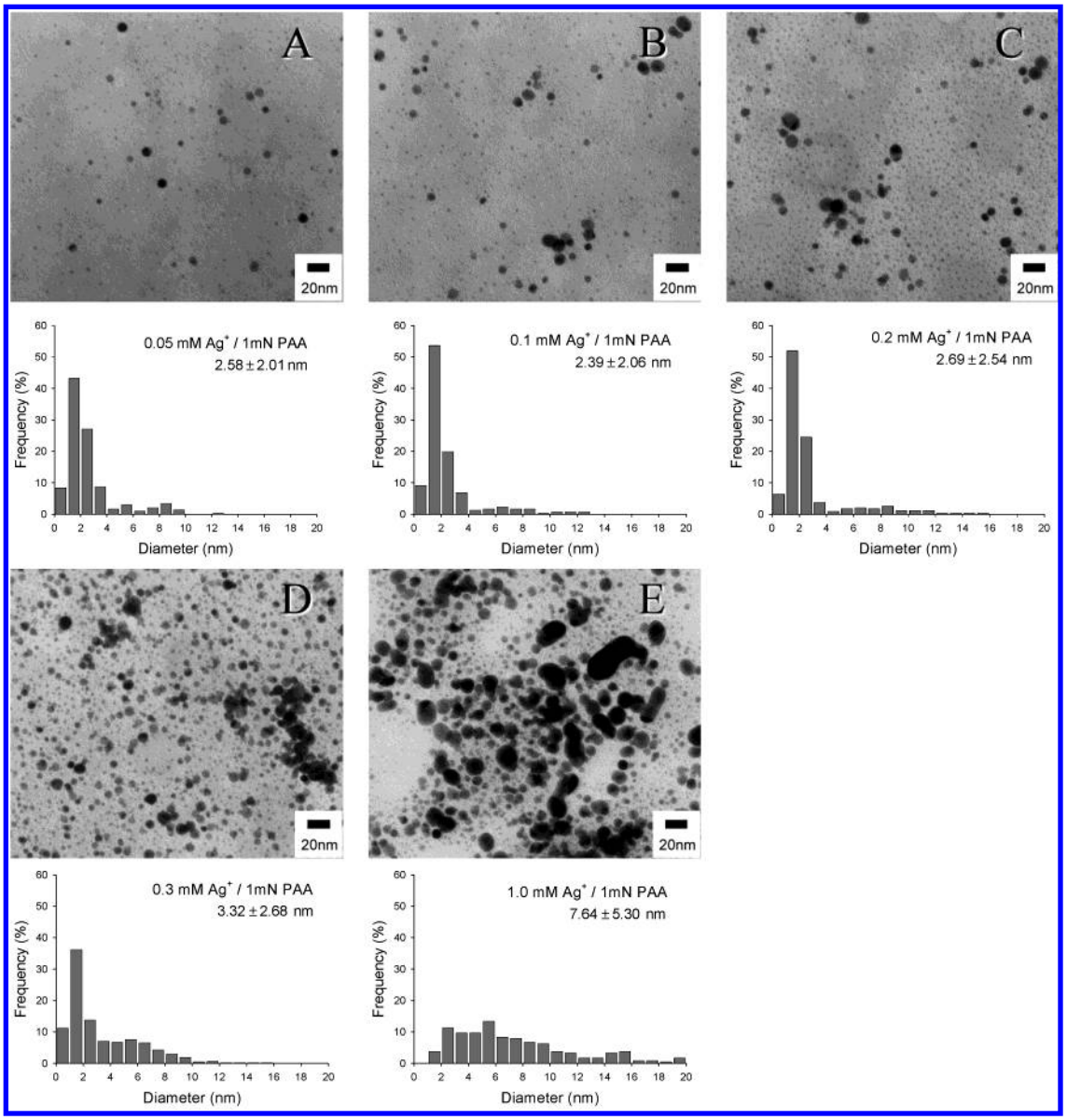

Figure 2. TEM images of metallic silver nanoparticles formed with [N] of PAA = 1 mM and different silver concentrations: (A) 0.05, (B) 0.1, (C) 0.2, (D) 0.3, and (E) 1.0 mM. The histograms under the micrographs show the particle size distributions.

borohydride at room temperature with the aid of ultrasonic vibration for 10 min. Finally yellow-orange transparent solutions of silver colloids were obtained.

Characterization with UV−Vis Spectrophotometer and TEM. The solutions before and right after reduction are measured at room temperature by a Jasco V-550 UV−vis spectrophotometer. Transmission electron micrographs are taken with a Zeiss 10C transmission electron microscope (TEM) operated at 80 kV accelerating voltage or a Hitachi Model HF-2000 field emission transmission electron microscope at 200 kV. Specimens are prepared by placing a drop of the colloidal solution onto 200-mesh copper or nickel grids coated with an

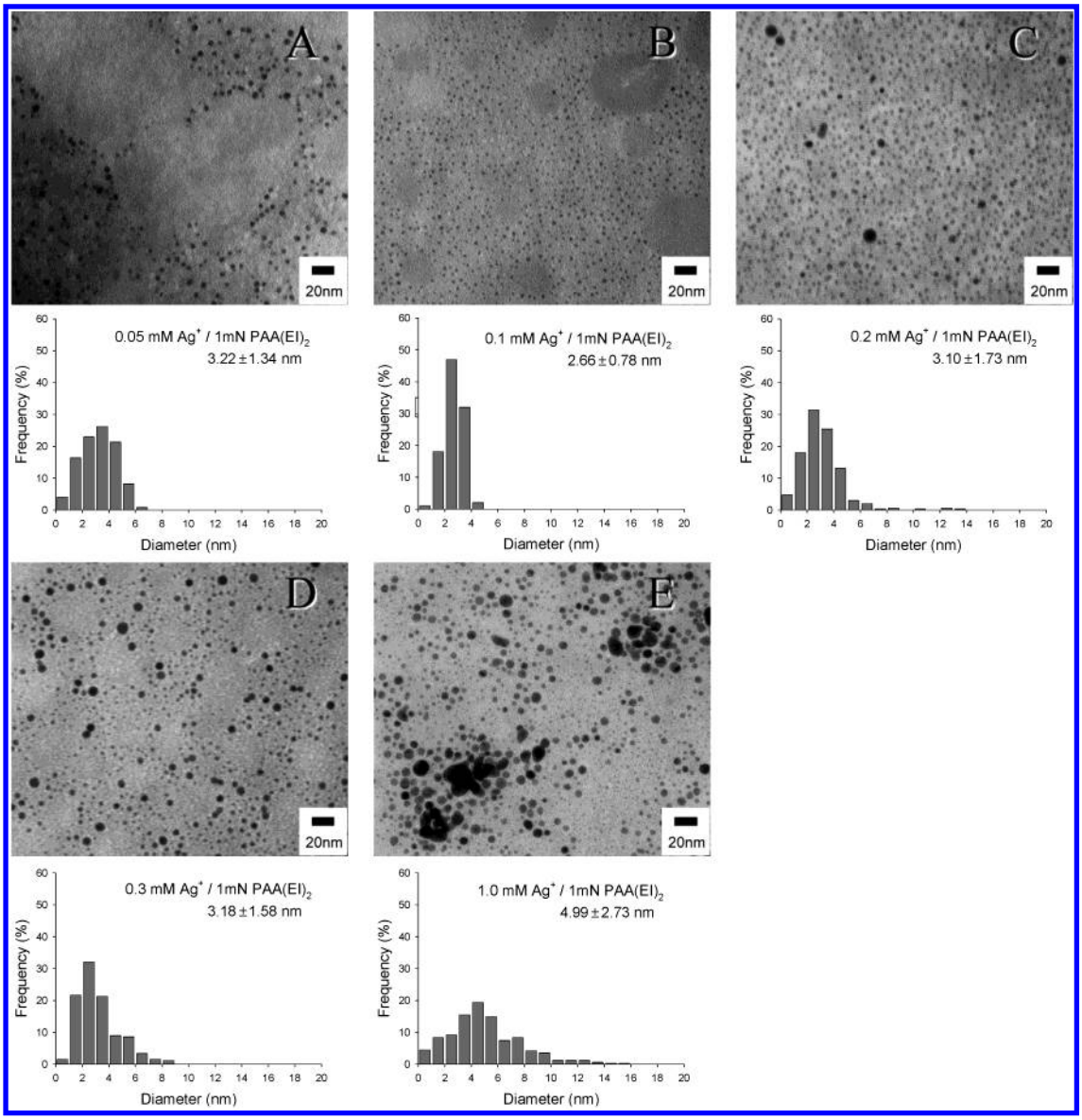

Figure 3. TEM images and corresponding histograms of metallic silver nanoparticles formed with [N] of $PAA(EI)_2$ = 1 mM and different silver concentrations: (A) 0.05, (B) 0.1, (C) 0.2, (D) 0.3, and (E) 1.0 mM.

amorphous Formvar carbon film and dried overnight at room temperature in a vacuum oven. The average particle sizes and size distributions are obtained on the basis of the measurement of at least 300 particles. The standard deviation σ of the size distribution is calculated from the equation as follows:

$$\sigma = \sqrt{\frac{\sum n_i (d_i - D)^2}{N - 1}}$$

where n_i is the number of particles having diameter d_i, N is the total number of particles counted, and the average diameter is computed from the equation $D = (\sum n_i d_i)/N$

Results and Discussion

UV−Vis Absorption Spectra of Silver Nanoparticles under $PAA(EI)_n$. Amino-containing dendrimer−Ag^+ complexes synthesized by direct complexation and characterized by electron paramagnetic resonance analysis evidenced the strong complexing between amino groups and Ag^+ ions.[17] Thus, $PAA(EI)_n$ can be expected to be highly effective as a polymeric chelating agent to Ag^+ ions. As excess $NaBH_4$ was added into the mixture solution, silver nanoparticles were formed simultaneously with the change in solution color from colorless to yellow. After storage in air for 6 months, the silver colloidal solution was still clear orange, and the UV−vis absorption spectra obtained after this storage period changed only very little.

Before reduction, Ag^+ ions show no absorptions in UV−vis spectra in $PAA(EI)_n$ aqueous solution due to its d^{10} configuration. After reduction, the absorption spectra of the silver nanoparticles passivated by PAA, $PAA(EI)_2$, and $PAA(EI)_{5.8}$ are shown in Figure 1a−c, respectively, which display strong absorption bands around 400 nm. These peaks arise from the surface plasmon absorption of silver colloids, because silver metals are known to have intense plasmon absorption bands in the visible region.[18,19] The shapes of these plasmon bands are almost symmetrical, suggesting the nanoparticles are well-dispersed and sphere-shaped since the aggregation of nanoparticles leads to red-shifted and broadened plasmon absorptions,[20] and the elongated nanoparticles bring on a splitting into two bands.[21] The absorption spectra are varied with increasing Ag^+ concentration as shown in Figure 1. The maximum absorbance at 400 nm increases linearly with increasing Ag^+ concentration, and the full bandwidth at half-maximum (FWHM) is slightly

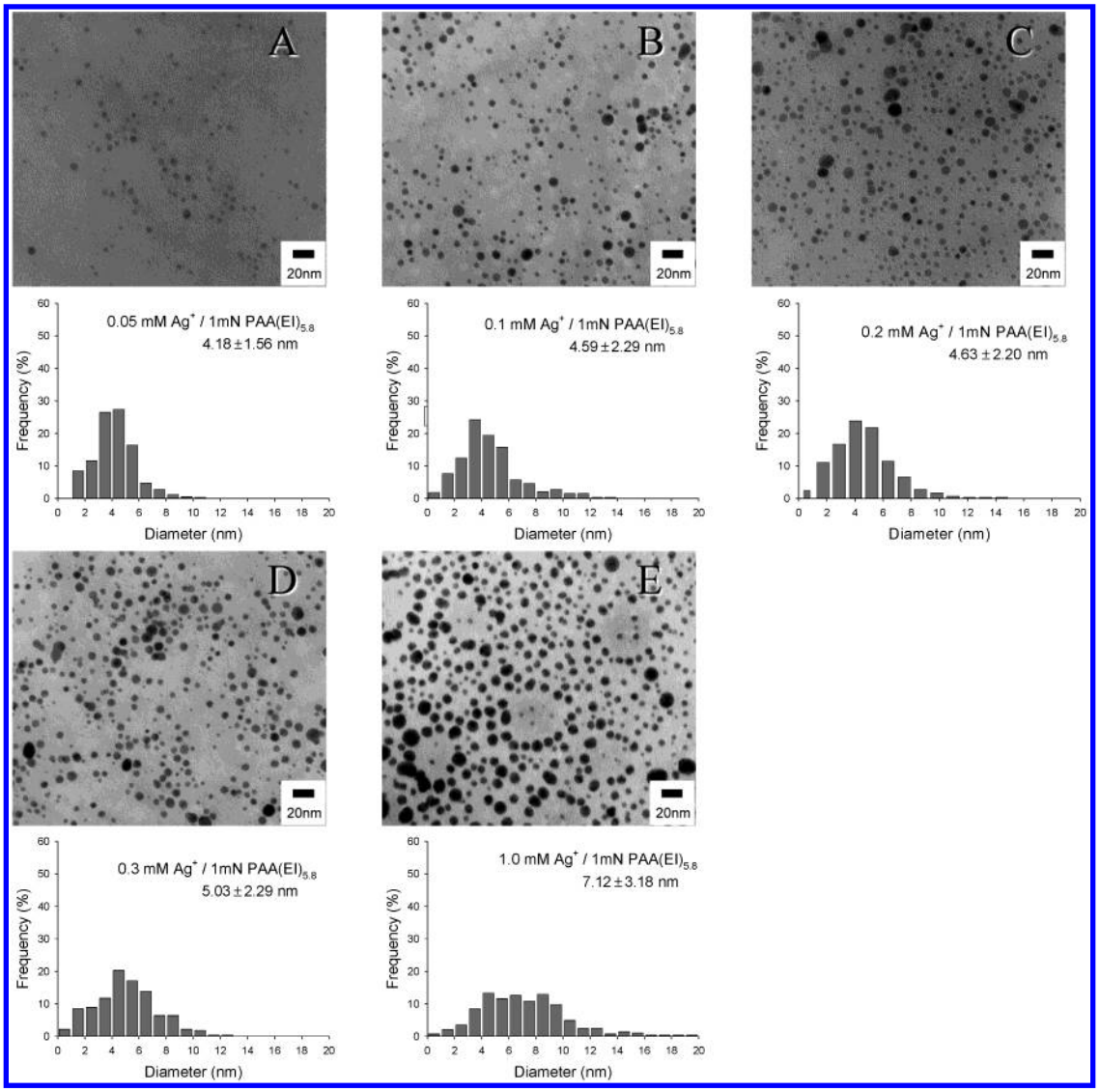

Figure 4. TEM images and corresponding histograms of metallic silver nanoparticles formed with [N] of $PAA(EI)_{5.8}$ = 1 mM and different silver concentrations: (A) 0.05, (B) 0.1, (C) 0.2, (D) 0.3, and (E) 1.0 mM.

enlarged. These results indicate that the silver nanoparticles tend to grow up as Ag^+ concentration increases.

Excluding the strong absorbance at 400 nm, the intensity of the peak at 290 nm also increases with Ag^+ concentration. On the earlier γ-irradiation study of aqueous silver nitrate solution, Ag clusters of a few atoms of Ag_n ($n = 1-3$, $4-7$, and $8-12$) were characterized with UV bands at 292, 325, and 370−380 nm, respectively.[22,23] Thus, the 290 nm peak observed in the present study can be reasonably attributed to the existence of oligomeric species with a general formula Ag_n^0 with $n < 4$.

The absorption spectra displayed in Figure 1 are so similar that the distinctions among these polymers can hardly be distinguished and are further investigated with the aid of transmission electron microscope as discussed later.

Architectural Effect of $PAA(EI)_n$ on the Formation of Silver Nanoparticles. To explore the effect of polymer architecture on particle formation, the Ag^+ concentrations are varied from 0.05 to 1 mM, and the polymer concentrations of $PAA(EI)_n$ are fixed at the same normality concentration (1 mN). The TEM images and the corresponding histograms of manual measurement of size distribution of silver nanoparticles prepared in the presence of PAA, $PAA(EI)_2$, and $PAA(EI)_{5.8}$ are shown in Figure 2, Figure 3, and Figure 4, respectively. Most of the nanoparticles are well-dispersed and sphere-shaped coinciding

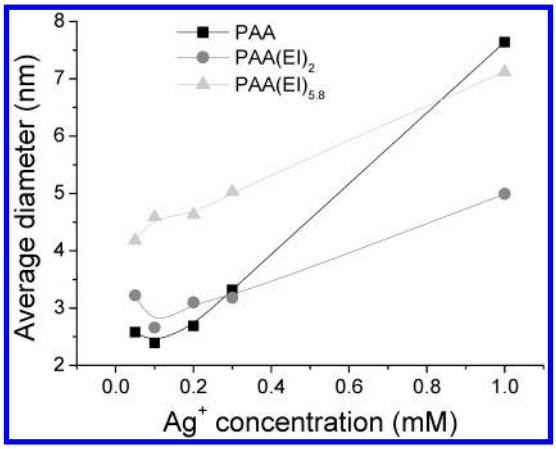

Figure 5. Relationship between the average particle diameters and Ag^+ concentrations with the concentration of $PAA(EI)_n$ fixed at 1 mN. The standard deviations for the plot of PAA, $PAA(EI)_2$, and $PAA(EI)_{5.8}$ are described in the corresponding histograms in Figures 2−4.

with the above-mentioned speculation of UV−vis absorption spectra. For PAA-protected silver nanoparticles, the agglomeration of small particles occurs as Ag^+ concentration increases (Figure 2). At high Ag^+ concentrations (1 mM/(1 mN) Ag^+/[N]), large and nonspherical agglomerated particles are formed

SCHEME 1: Schematic Representation of the Structure-Dependent PAA(EI)$_n$-Protected Silver Nanoparticles

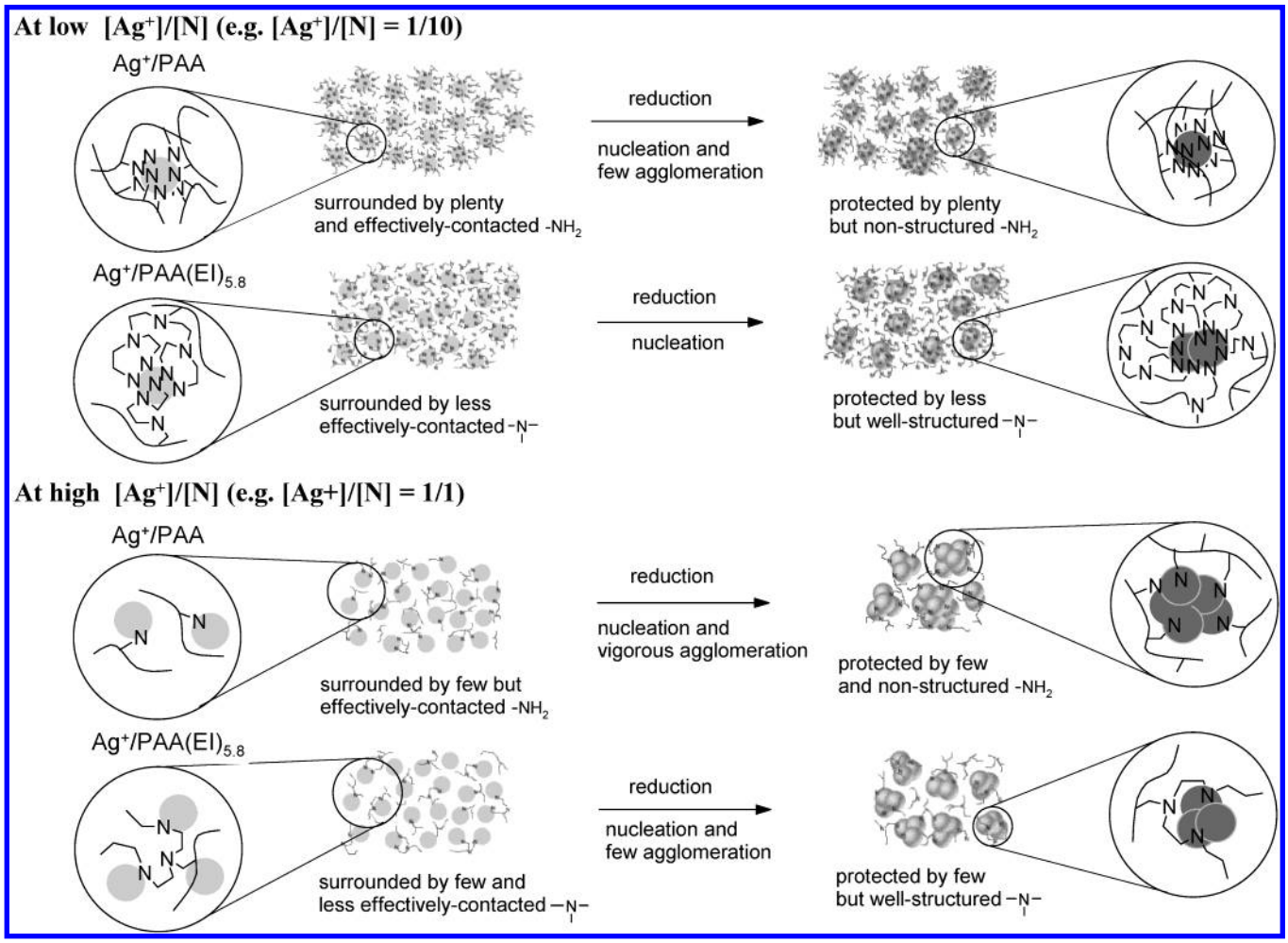

in the majority, as shown in Figure 2E. In comparison with this, small particles accompanied with agglomeration for PAA-(EI)$_2$ (Figure 3E) and larger particles without agglomeration for PAA(EI)$_{5.8}$ (Figure 4E) are observed. These results indicate that the order of increasing stabilization for protecting silver nanoparticles is PAA(EI)$_{5.8}$ > PAA(EI)$_2$ > PAA.

The average particle sizes and standard deviations computed from these TEM micrographs are listed in their histograms. At lower Ag^+ concentration such as 0.05 mM, the order of increasing average diameter is PAA (2.58 nm) < PAA(EI)$_2$ (3.22 nm) < PAA(EI)$_{5.8}$ (4.18 nm), but for standard deviation the order is mainly PAA(EI)$_2$ < PAA(EI)$_{5.8}$ < PAA. The average particle sizes increase with the increasing Ag^+ concentration coinciding with the inference from plasmon absorption spectra shown in Figure 1. In Figure 5, the average particle diameter is plotted versus the Ag^+ concentrations. The increasing rate of particle size as a function of Ag^+ concentration can be obtained from the slope of the linear region of these curves. Obviously, the rates for PAA(EI)$_2$ and for PAA(EI)$_{5.8}$ are similar, but the rate for PAA is much higher than that for PAA-(EI)$_2$ or PAA(EI)$_{5.8}$, though the initial point for PAA is lower. PAA is more sensitive to the increasing Ag^+ concentration, indicating that PAA is not so effective in protecting nanoparticles as PAA(EI)$_2$ or PAA(EI)$_{5.8}$. Obviously, the architectural effects gradually become more important above sufficiently high Ag^+ concentrations. PAA(EI)$_{5.8}$ has longer polyethyleneimine chains which perform a better steric effect in stabilizing silver nanoparticles but less effectively contact with Ag^+ (as discussed in Scheme 1 below). As shown in Figure 5, for Ag^+ concentration up to 1.0 mM, the ability to constrain the particle growth for PAA(EI)$_{5.8}$ is close to that for PAA(EI)$_2$.

In the presence of PAA, the growth of stabilized particles ends in a critical size of 3 nm, while the poorly stabilized ones develop to form larger particles (5−10 nm) and further agglomerate as shown in Figure 2A−2C. This also can be demonstrated from the multidistribution in their histograms. At high Ag^+ concentrations, the insufficiency of protecting amine groups leads to vigorous agglomeration and irreversible flocculation observed in Figure 2E.

On the other hand, well-stabilized particles with a critical size of around 6 nm (Figure 4A) form predominantly under the protection of PAA(EI)$_{5.8}$. Even at higher Ag^+ concentrations, the stabilization is so strong that less agglomeration occurs and lower standard deviations are obtained, as shown in Figure 4E. As for PAA(EI)$_2$, at low Ag^+ concentrations, it results in the well-stabilized and small particles of 4−5 nm without agglomeration (Figure 3A,B), possessing both the merits of PAA and PAA(EI)$_{5.8}$. At sufficiently high Ag^+ concentration, however, it cannot protect the Ag particles as effectively as PAA(EI)$_{5.8}$ so that multidistribution appears and agglomeration occurs.

PAA(EI)$_{5.8}$ exhibits better protective effect than PAA; however, the critical size of PAA(EI)$_{5.8}$-stabilized particles is larger than that of PAA. The average diameters of the particles obtained under PAA are smaller at low Ag^+ concentrations but larger at high Ag^+ concentrations than those under PAA(EI)$_{5.8}$. These results are explained with the following mechanism schematically depicted in Scheme 1. According to the IR results reported by Manna et al.,[24] both 1° amine and 2° amine complex

with Ag^+ to induce an IR shift which is more remarkable for the former. Thus, both the amino groups on PAA and those of poly(ethyleneimine) on $PAA(EI)_{5.8}$ can be expected to interact with Ag^+; however, the amino groups on PAA are naked on the flexible chain, whereas a portion of amino groups on $PAA(EI)_{5.8}$ are 2° or 3° amines which are steric-hindranced on the strained hyperbranch poly(ethyleneimine). On average, amino groups on PAA can be considered to more effectively contact with Ag^+ than those on $PAA(EI)_{5.8}$ parallel to the trend of IR shift and the phenomena of terminal groups in dendrimers reported by Manna et al. Thus, at the low ratio of silver ions and amine groups, Ag^+ ions are surrounded by plenty of effectively contacted primary amines in the presence of PAA, but by a lower amount of effectively contacted amino groups in the presence of $PAA(EI)_{5.8}$. After reduction, the particles are surrounded by more plentiful amino groups of PAA to form small ones with diameters of 1−3 nm; however, a few agglomerations occur because the nonstructured amino groups on flexible PAA polymer backbone do not provide sufficient protective effect to prevent particles from agglomerating. As for $PAA(EI)_{5.8}$, the effectively contacted amine groups on the pendent ethyleneimine groups are less but effectively protect the silver particles leading to larger but well-stabilized nanoparticles in 2−6 nm. At high $[Ag^+]/[N]$ ratio, a lower amount of the nonstructured amino groups of PAA provide very poor stabilization, resulting in irreversible agglomeration, whereas the well-structured ethyleneimine groups of $PAA(EI)_{5.8}$ perform steric effect to shield these silver nanoparticles from agglomeration.

Conclusions

UV−vis spectroscopic studies reveal the formation of silver nanoparticles, and the TEM images show the distinct features of the particle formation demonstrating the architectural effects of these polymers. The silver nanoparticles prepared in the presence of PAA, $PAA(EI)_2$, and $PAA(EI)_{5.8}$ are most well-dispersed and sphere-shaped coinciding with the speculation of UV−vis absorption spectra. The order of ability to prevent agglomeration of silver particles is $PAA(EI)_{5.8} > PAA(EI)_2 >$ PAA, and the order of constraint on particle growth is $PAA(EI)_{5.8} \approx PAA(EI)_2 >$ PAA. Generally speaking, $PAA(EI)_2$-protected silver particles possess both advantages of stabilization and narrow distribution, but $PAA(EI)_{5.8}$ displays the best stabilizing property at higher Ag^+ concentrations.

Acknowledgment. The authors would like to thank the National Science Council, Taipei, ROC, for their generous financial support of this research.

References and Notes

(1) Lisiecki, I.; Pileni, M. P. *J. Am. Chem. Soc.* **1993**, *115*, 3887.
(2) Wang, C. C.; Chen, D. H.; Huang, T. C. *Colloid Surf., A* **2001**, *189*, 145.
(3) Chen, D. H.; Chen, Y. Y. *Mater. Res. Bull.* **2002**, *37*, 801.
(4) Yang, H.; Wang, Z.; Song, L.; Zhao, M.; Chen, Y.; Dou, K.; Yu, J.; Wang, L. *Mater. Chem. Phys.* **1997**, *47*, 249.
(5) Haruta, M.; Yamada, N.; Kobayashi, T.; Iijima, S. *J. Catal.* **1989**, *115*, 301.
(6) Zhang, Z.; Zhang, L.; Wang, S.; Chen, W.; Lei, Y. *Polymer* **2001**, *42*, 8315.
(7) Yanagihara, N.; Tanaka, Y.; Okamoto, H. *Chem. Lett.* **2001**, 796.
(8) Stoeva, S.; Klabunda, K. J.; Sorensen, C. M.; Dragieva, I. *J. Am. Chem. Soc.* **2002**, *124*, 2305.
(9) Curtis, A. C.; Duff, D. G.; Edwards, P. P.; Jefferson, D. A.; Johnson, B. F. G.; Kirkland, A. I.; Wallace, A. S. *Angew. Chem., Int. Ed. Engl.* **1988**, *27*, 1530.
(10) Morris, T.; Copeland, H.; Szulczewski, G. *Langmuir* **2002**, *18*, 535.
(11) Balogh, L.; Tomalia, D. A. *J. Am. Chem. Soc.* **1998**, *120*, 7355.
(12) (a) Crooks, R. M.; Zhao, M.; Sun, L.; Chechik, V.; Yeung, L. K. *Acc. Chem. Res.* **2001**, 34, 3, 181. (b) Zhao, M.; Crooks, R. M. *Chem. Mater.* **1999**, *11*, 3379.
(13) (a) Esumi, K.; Suzuki, A.; Aihara, N.; Usui, K.; Torigoe, K. *Langmuir* **1998**, *14*, 3157. (b) Esumi, K.; Torigoe, K. *Prog. Colloid Polym. Sci.* **2001**, *117*, 80. (c) Garcia, M. E.; Baker, L. A.; Crooks, R. M. *Anal. Chem.* **1999**, *71*, 256.
(14) Manna, A.; Imae, T.; Aoi, K.; Okada, M.; Yogo, T. *Chem. Mater.* **2001**, *13*, 1674.
(15) Kuo, P. L.; Ghosh, S. K.; Liang, W. J.; Hsieh, Y. T. *J. Polym. Sci., Part A: Polym. Chem.* **2001**, *39(17)*, 3018.
(16) Zhao, M.; Sun, L.; Crooks, R. M. *J. Am. Chem. Soc.* **1998**, *120*, 4877.
(17) Ottaviani, M. F.; Valluzzi, R.; Balogh, L. *Macromolecules* **2002**, *35*, 5105.
(18) Henglein, A. Giersig, M. *J. Phys. Chem. B* **1999**, *103*, 9533.
(19) Petit, C.; Lixon, P.; Pileni, M. P. *J. Phys. Chem.* **1993**, *97*, 12974.
(20) Zheng, J.; Stevenson, M. S.; Hikida, R. S.; Gregory Van Patten, P. *J. Phys. Chem. B* **2002**, *106*, 1252.
(21) Mayer, A. B. R.; Mark, J. E. *Polymer* **2000**, *41*, 1627.
(22) Mostafavi, M.; Delcourt, M. O.; Keghouche, N.; Picq, G. *Radiat. Phys. Chem.* **1992**, *40*, 445.
(23) Mostafavi, M.; Delcourt, M. O.; Picq, G. *Radiat. Phys. Chem.* **1993**, *41*, 453.
(24) Manna, A.; Imae, T.; Iida, M.; Hisamatsu, N. *Langmuir* **2001**, *17*, 6000.